Backscattering study and theoretical investigation of planar channeling processes. I. Experimental results*

F. Abel, G. Amsel, M. Bruneaux, C. Cohen, and A. L'Hoir
Groupe de Physique des Solides de l'Ecole Normale Supérieure, Tour 23, 2 Place Jussieu, 75221 Paris Cedex 05, France
(Received 24 March 1975; revised manuscript received 9 June 1975)

Backscattering experiments in planar channeling have been performed on iron single crystals with 1.9-MeV ^{4}He beams; these conditions having been chosen for optimal study of the structure of the spectra. Both for the (110) and (100) planes five equally spaced yield maxima are clearly resolved, the maxima damping out at lower energies. Spectra were also registered at various angles of incidence φ_0 with respect to the planes. Yield maxima are observed up to values of φ_0 twice the half-width at half-minimum $\psi_{1/2}$ of an angular scan across the plane [$\psi_{1/2} = 18'$ for the (110) plane]. Except for the first two peaks, these maxima have the same spacing as in the aligned spectrum. They appear to be due to particles belonging to a well-defined transverse energy interval. The mean stopping power for these particles is close to the random stopping power and the mean half-wavelength of their oscillating trajectories in the planar channels calculated from the results is $\lambda = 380$ Å for the (110) plane and $\lambda = 320$ Å for the (100) plane. For $\varphi_0 > 1.2\psi_{1/2}$, the yield on the first maximum is greater than the random yield, reaching ~ 1.6 times the latter for $1.4\psi_{1/2} < \varphi_0 < 1.8\psi_{1/2}$. The shoulder effect in the angular scans, as observed for various depths, is clearly related to the yield maxima and hence depends strongly on the position and width of the depth interval chosen. The meaning and validity of the assumption of statistical equilibrium for planar channeled particles are discussed in light of the results.

INTRODUCTION

Particles undergoing planar channeling present only one degree of freedom with respect to the crystal planes, in contrast to the axial case. For low enough transverse energies, $E_\perp$, the individual trajectories are hence confined within two well-defined planes and present a nearly periodic oscillatory character. The theoretical description of such a process may be restricted to two dimensions; the ensuing simplification is considerable and a realistic analytical treatment of this case seems not out of reach.

The oscillatory effects were evidenced experimentally and studied in detail in transmission-type experiments.[1-4] They were first reported in backscattering experiments on tungsten using a magnetic spectrometer by Bøgh,[5] who observed a structure in the planar aligned spectra. Strong regularly spaced maxima in such spectra were observed by the present authors on iron using 1.9-MeV ^{4}He beams and semiconductor detectors[6]; at least five maxima were clearly resolved and their presence was assigned to an oscillatory-type motion of the planar channeled particles. A stochastic interpretation of these observations was presented in Ref. 7. Poizat and Remillieux[8] also observed a structure on gold thin crystals while, more recently, Van der Weg *et al.*[9] resolved four maxima in spectra registered with 120-keV protons on silicon.

In contrast to transmission-type experiments, backscattering-type measurements give information focused on the trajectories of those particles which may move very near the planes, i.e., with high transverse energies $E_\perp$. From the observed spectra, the nuclear encounter probabilities with the atoms of the crystal as a function of depth may be deduced and compared to calculations. These probabilities have been computed by Barrett[10,11] using Monte Carlo methods for axial and planar channeling. In both cases these probabilities exhibit a strongly oscillatory behavior which progressively damps out with depth. However, the maxima are much more pronounced, more regularly spaced, and the damping much slower for planar channeling. One major consequence of the oscillatory features of the particle motion is that the probability density of the particles across the planar channels, i.e., the flux, depends on the penetration depth. Consequently, the nuclear encounter probability with a nonsubstitutional impurity is also expected to vary strongly with depth. Various computer simulations have been performed to calculate the probability density of the particles in the channels.[12,13] The results have been applied to interpret lattice location experiments.[14,15]

The purpose of the present work was to experimentally observe the oscillatory effects in planar channeling in the best conditions and to attempt the elaboration of a theoretical interpretation of the results, as comprehensive as possible. Iron bombarded with 1.9-MeV ^{4}He ions was chosen as the best case; the results are reported in this paper. Paper II presents full calculations in the absence of statistical effects, when the particle is considered as an unperturbed oscillator moving in a static continuum potential: valuable qualitative information is obtained in this way. In Paper III more realistic models of planar channeling will be considered, which take into account the statis-

tical effects of multiple scattering and of thermal vibrations, by resorting to the theory of stochastic processes. In all these calculations it will be attempted to use analytical methods which shed more light on basic principles than Monte Carlo methods, although the latter may be carried out without approximations and might hence be quantitatively more precise. In some cases electronic simulation of the processes will also be used. The experimental results will be compared to the theoretical predictions; in particular, the meaning and validity of the classical concept of statistical equilibrium, as applied to planar channeling phenomena, will be examined in light of the results of both experiments and theory. The consequences for lattice location experiments will be emphasized. Preliminary reports on this work are contained in Refs. 16–18.

EXPERIMENTAL

The measurements were carried out using the 2-MeV Van de Graaff generator, the beam handling system and experimental facilities described in Refs. 19 and 20. The goniometric chamber used here is schematized in Fig. 1. The horizontally revolving stage has an angular travel of $\pm 45°$. This stage bears a stage R rotating in a vertical plane with an angular travel of $\pm 180°$. These two movements are driven by stepping motors. A thermally insulated sample holder is supported by an X-Y table which allows one to translate the samples parallel to themselves by ± 10 mm in each direction. The table is fixed on a two axis goniometer of the compass-type with maximum angular travels of $\pm 3°$ around two perpendicular axes.

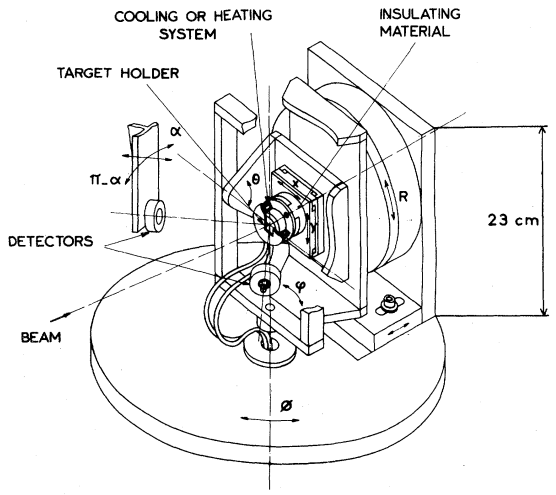

FIG. 1. Schematic diagram of the goniometric chamber.

The latter movements are driven by small dc motors coupled to ten-turn potentiometers, a numerical display indicating the positions. The compass-type goniometer is used to align a crystallographic axis with the rotation axis of the vertical stage R. In this way the angle between the beam and the crystallographic axis may be defined by the position of the horizontal stage and remains constant while the sample is rotated by the vertical stage R. The alignment between the incident beam and a crystallographic axis or plane is controlled within 1′ precision; the translations of the samples, which are very useful to reduce the effects of radiation damage on the results keep the alignments within this precision. The sample holder is surrounded by a hollow metallic ring. The cavity may contain a resistor for heating the sample or may be coupled to a liquid-nitrogen circulation system for cooling. In this way the samples may be heated up to 600 °C or cooled down to − 120 °C, while full freedom of all movements is preserved.

Two detectors may be placed in the chamber at adjustable distances from the samples. These detectors may be cooled to − 50 °C. The detection angles may be changed independently from the outside without opening the chamber from 115° to 175°. The limiting vacuum obtained in the chamber coupled to a turbomolecular pump and using a liquid air trap is 5×10^{-7} Torr. The whole chamber is well insulated and acts as a Faraday cup. Using the Brookhaven Instruments Model 1000A low-impedance current integrator, beam currents around 10 nA may be measured in this way without significant errors on the total incident charge. For beam currents around 1 nA, pickup problems arise, but in these experiments the beam currents were usually around 30 nA.

The experiments were performed with a 1.9-MeV $^4He^+$ beam, the beam divergence being less than 0.5 mrad. The backscattered particles were analyzed at 165° or 120° with 25-mm^2 Ortec surface-barrier detectors with about 1000 Ω cm resistivity. In order to minimize kinematic effects, especially for detection at 120°, a stainless-steel diaphragm was used with a vertical rectangular hole of 1.5×4 mm. The detector was placed 8 cm from the sample, the subtended solid angle being hence about 1 msr. The energy resolution was about 15 keV, the noise linewidth being 6 keV, with the 109A Ortec preamplifier used. The corresponding depth resolution was about 150 Å for detection at 165° and 100 Å for detection at 120° for incoming and outcoming particles in random directions. The maximum kinematic effect for backscattering at the surface was about 4 keV, i.e., rather small compared to the energy resolution.

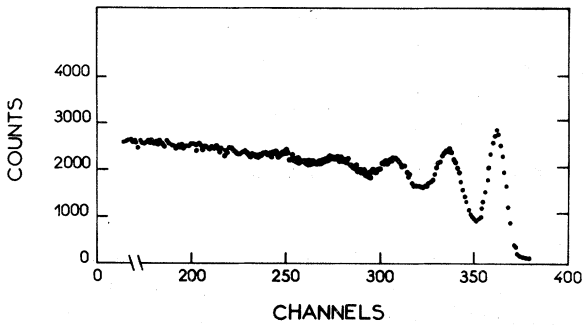

FIG. 2. (100) planar aligned spectrum at 5° off the [001] axis for a 1.9-MeV ^{4}He beam, $\theta_{lab}=120°$, 2.24 keV/channel.

RESULTS

A. Choice of the experimental conditions

A typical (100) aligned spectrum is presented in Fig. 2. It exhibits at least four clearly resolved maxima behind the surface peak. The energy spacing between two consecutive maxima is fairly constant, increasing only by a few percent towards low energies. The (110) aligned spectrum shown in Fig. 3 exhibits the same features. These two spectra were registered at 5° off the [001] axis.

The planar-aligned backscattering spectra observed by many authors appeared to be monotonous. This is due to the fact that in most experiments the depth resolution was large compared to the mean half-wavelength λ of the trajectories of the particles contributing to the maxima of the yield. In order to observe a structure in the backscattering spectra, one has to optimize the ratio λ/R_x, R_x being the depth resolution. This implies that the expression $\lambda(dE/dx)/R_E$, where R_E is the energy resolution, must be maximized. In our case, R_E is set mainly by the use of surface-barrier detectors and the optimization bears only on the choice of the crystal and of the nature and energy of the particles.

When the incident beam is parallel to a crystallographic plane, the particles which may be backscattered enter the crystal with small impact parameters with respect to the planes. Their mean half-wavelength λ is then of the order of D/ψ_c, where D is the distance between two consecutive planes and ψ_c is the angle of the trajectories of these particles at the channel center. In the approximation of conserved transverse energy, ψ_c is of the order of $[U(0)/E]^{1/2}$, where $U(0)$ is the planar potential at the plane, the origin of the potential being taken at the channel center and E is the energy of the particles. Finally, ψ_c is proportional to $(Z_1 Z_2 ND/E)^{1/2}$, where Z_1 and Z_2 are the atomic numbers of the incident particles and of the lattice atoms and N the number of lattice atoms/cm^3. Hence,

$$\lambda \sim (E D/Z_1 Z_2 N)^{1/2} . \quad (1)$$

To have the best chance to observe a structure in a backscattering spectrum, one should hence maximize the expression

$$\frac{dE}{dx} (E D/Z_1 Z_2 N)^{1/2}/R_E . \quad (2)$$

1. Choice of the nature and energy of the incident particles

According to Eq. (2), the particle-dependent quantity

$$\mu = \frac{dE}{dx}\left(\frac{E}{Z_1}\right)^{1/2} \Big/ R_E \quad (3)$$

must be maximum. In the energy range accessible to our 2-MeV accelerator, ^{4}He ions appear to be the best particles. In this energy domain the numerator of expression (3) is 6 to 9 times greater for the case of helium than for deuterons or protons. The better energy resolution (10 keV for proton as compared to 15 keV for helium with usual surface barrier detectors in the 0.5- to 2-MeV energy range) for protons and deuterons is, of course, too small to offset this large factor. On the other hand, the depth resolution $(dE/dx)/R_E$ is very similar for helium and heavier particles (carbon, nitrogen, oxygen) in the energy domain of interest, the gain in stopping power for heavier particles being compensated by the rather poor energy resolution of the surface barrier detectors for the latter (45 keV for 2-MeV ^{12}C). As μ decreases when Z_1 is increased, these particles are less favorable than ^{4}He. Lithium ions are likely to be slightly more favorable than ^{4}He but such beams are rarely available.

In Table I we report the variation of μ as a func-

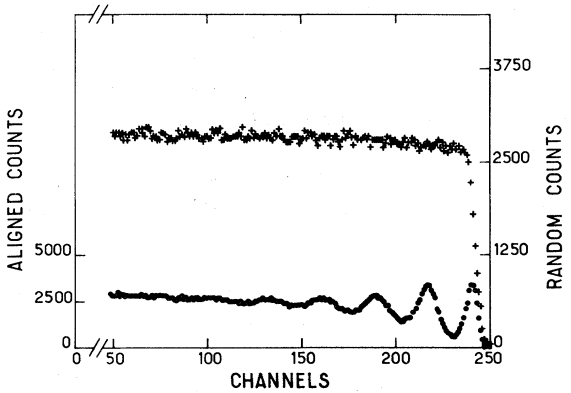

FIG. 3. (110) planar aligned spectrum at 5° off the [001] axis and corresponding random spectrum for a 1.9-MeV ^{4}He beam. $\theta_{lab}=120°$, 2.61 keV/channel. The random spectrum is normalized so as to show the extinction ratio.

TABLE I. Choice of the best energy to observe a structure in a planar aligned backscattering spectrum for a ^{4}He beam. μ must be maximized.

E MeV	0.5	1	1.5	1.9	2	2.5	3	4	5
μ (arbitrary units)	19	25.6	28.6	29.9	30.1	30.9	31.4	31.6	31.6

tion of energy for helium ions. This expression approaches practically its maximum value above 1.5 MeV. For higher energies the value of μ remains nearly constant the stopping power decreasing like $E^{-1/2}$ and λ increasing like $E^{1/2}$. In conclusion, an incident beam of ~2-MeV helium ions which can be obtained easily with our accelerator is near the optimum when surface-barrier detectors are used for energy analysis.

The preceding reasoning was based on rather high values of R_E. For low-energy protons (for instance near 100 keV, where the stopping power is maximum), energy resolutions as low as 2 keV were reported using cooled detectors and, in principle, electrostatic energy analysis could further reduce this figure. In this case R_E must be calculated taking into account energy straggling effects. Let us consider this case for silicon crystals in which Van der Weg *et al.*[9] actually observed in planar channeling three maxima behind the surface peak with 2.8-keV energy resolution for a 120-keV incident proton beam. The variance σ_S^2 of the straggling is given approximately by

$$\sigma_S^2 = Z_1^2 Z_2 Nl \times 2.6 \times 10^{-19}\ , \tag{4}$$

where l is the pathlength in a random direction given in cm, σ_S being expressed in keV. In silicon the corresponding energy spread [full width at half-maximum (FWHM)] is, for particles emerging from a depth 3λ (taking a mean value for λ around 200 Å and σ_S^2 near the random value for ingoing particles) around 3.5 keV. Hence an R_E of about 3 keV is reasonable for comparison with the ^{4}He case even if the actual resolution is much better. For crystals with higher Z_2 the situation is poorer; for example R_E is equivalent to 5 keV for iron under the same assumptions. In the silicon case, the energy resolution for 2-MeV ^{4}He ions emerging from a depth 3λ is near 19 keV taking the straggling into account and assuming an energy resolution of 15 keV at zero depth. With these figures the value of μ is still 1.4 times higher for 2-MeV ^{4}He ions than for 120-keV protons. The use of a low-energy proton beam presents another disadvantage as compared to MeV ^{4}He beams; for the first beam the mean energy loss over a penetration depth corresponding to a few λ is not small as compared to the incident energy, this leading to difficulties in data reduction and interpretation.

2. *Choice of the crystal*

According to Eq. (2) the crystal-dependent quantity

$$\nu = \frac{dE}{dx} \times \left(\frac{D}{Z_2 N}\right)^{1/2} \tag{5}$$

must be maximized. ν is reported in Table II for several targets, in arbitrary units normalized to the iron value. The incident beam was taken as 2-MeV ^{4}He and, for each target, the best atomic plane, i.e., corresponding to the maximum value of D, is considered. The results indicate that transition metals and particularly iron appear to be the most convenient targets for observing the phenomenon. Table II also reports the values of ρ for different targets, ρ being the rms of the thermal vibration amplitude perpendicularly to the planes. ρ appears to be relatively small for iron, the thermal vibration amplitude being only smaller in tungsten and molybdenum. The multiple scattering in iron is hence presumably smaller than in most crystals and the oscillating trajectories are expected to remain nearly periodic up to larger depths. A structure in the backscattering spectra in iron should hence extend over a rather wide energy range corresponding to a higher number of resolved maxima.

TABLE II. Choice of the target to optimize the observation of a structure in a planar aligned backscattering spectrum. ν has to be maximum and ρ minimum.

Target	Al	Si	V	Fe	Ni	Mo	Ag	Nb	W	Au
ν (arbitrary units)	0.85	0.78	0.92	1	0.92	0.83	0.68	0.78	0.79	0.78
ρ (Å) at 300 °K	0.102	0.077	0.0710	0.0617	0.0651	0.0472	0.0899	0.0657	0.0422	0.0918

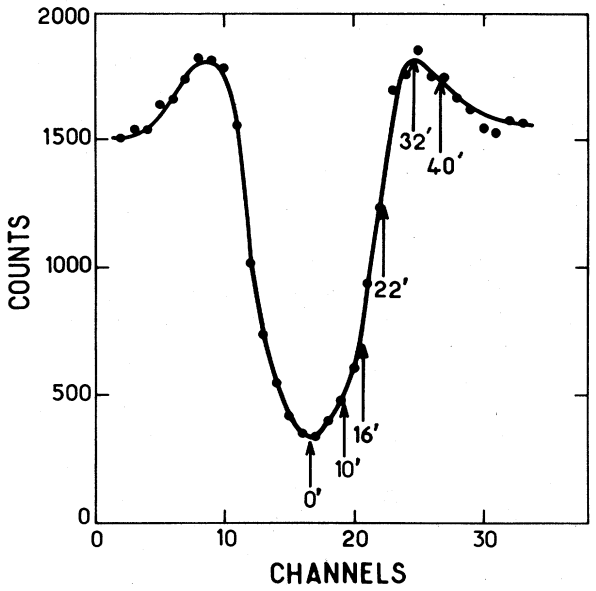

FIG. 4. Angular scan across the (110) plane. 4' per channel. The arrows indicate values of φ_0 for which some of the spectra in Figs. 5 and 6 were recorded. This scan was obtained for an energy window corresponding to the first 500 Å of the crystal.

B. Data

The samples were iron crystals (001) oriented. After electrochemical polishing,[21] they were placed in the goniometric chamber and their surface-oxygen content was first measured by nuclear microanalysis using the $^{16}O(d, p)^{17}O^*$ nuclear reaction.[19] They appeared to be covered by an oxyde layer containing from 10×10^{15} to 20×10^{15} oxygen atoms/cm^2 according to the experiments. In some experiments the samples were heated up

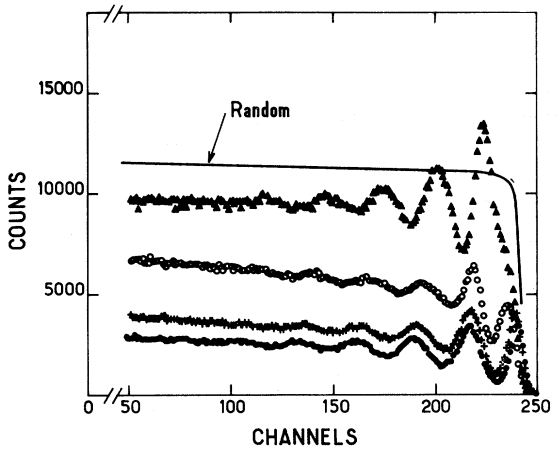

FIG. 5. Spectra registered at various angles of incidence φ_0 with respect to the (110) plane for a 1.9-MeV ^{4}He beam. $\theta_{lab}=120°$, 2.61 keV/channel. ●, $\varphi_0=0'$; +, $\varphi_0=10'$; ○, $\varphi_0=16'$; △, $\varphi_0=22'$.

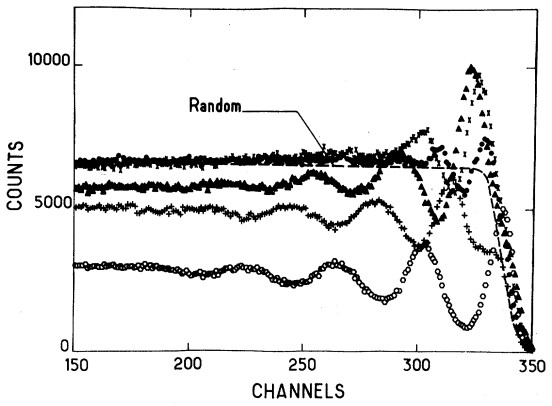

FIG. 6. Spectra registered at various angles of incidence φ_0 with respect to the (110) plane for a 1.9-MeV ^{4}He beam. $\theta_{lab}=120°$, 2.24 keV/channel. ○, $\varphi_0=0'$; +, $\varphi_0=20'$; ▲, $\varphi_0=24'$; ×, $\varphi_0=32'$; ●, $\varphi_0=40'$.

to 500° in the goniometric chamber at a residual pressure of 2×10^{-6} Torr for 30 min. After this annealing the remaining oxygen content was ~5 $\times10^{15}$ oxygen atoms/cm^2 (i.e., about 10 Å assuming Fe_2O_3). The decrease of the oxygen content after annealing could be due to thermal decomposition of volatile adsorbed species on the surface layer such as carbonates.

Spectra were registered at various angles of incidence φ_0 with respect to the (110) plane. Figure (4) shows an angular scan across this plane obtained by integrating the yield corresponding to the first two peaks of an aligned spectrum. The half-width at half-minimum as measured on this scan is $\psi_{1/2}=18'$. Figures 5 and 6 represent the spectra obtained at various φ_0 in two sets of experiments. Some of the φ_0 corresponding to spectra in Figs. 5 and 6 are indicated on the angular scan of Fig. 4. Strong maxima are observed on all spectra up to $\varphi_0=40'$. Up to $\varphi_0=24'$, the energy interval between two consecutive maxima is fairly constant except for the first two peaks and equal to the energy interval measured on the aligned spectrum. The first maximum, i.e., the so-called "surface peak," is shifted towards lower energies, i.e., towards greater penetration depths, as φ_0 is increased. It should be emphasized that for $22' \leqslant \varphi_0 < 32'$ the yield on the first maximum is higher than the random yield, while the uniform level reached at low energies is still markedly lower than the random level. For $\varphi_0=32'$ and $\varphi_0=40'$, the random level is reached at low energies but the high-energy part of the spectra still exhibits two or three well-resolved maxima corresponding to yields greater than the random yield. A fair random spectrum, i.e., with only very small noticeable structure on the high-energy part, could be registered at $\varphi_0=50'$.

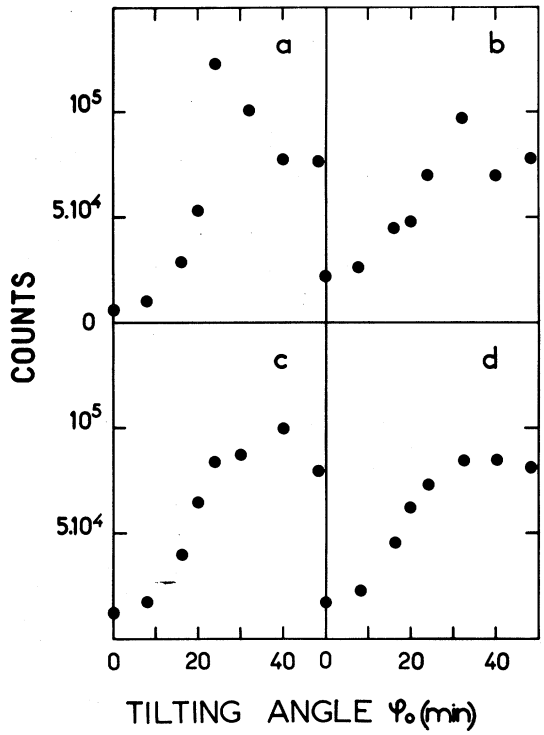

FIG. 7. Angular scans at various depths x extracted from Fig. 6, 4' per channel. (a) $x=160$ Å, (b) $x=370$ Å, (c) $x=550$ Å, (d) $x=1400$ Å. The integration depth is ~100 Å.

Various angular scans were extracted from the spectra of Fig. 6. The yield as a function of tilting angle was obtained by integration over energy windows centered at various energies in the spectra. The width of the energy windows was chosen of the order of the energy resolution, i.e., $\simeq 15$ keV. The energies on which these windows were centered correspond, respectively, to penetration depths of 160, 370, 550, and 1400 Å, applying the energy to depth conversion that will be discussed below. The angular scans obtained are reported in Fig. 7. The statistics being very good, the details of the shape of these scans are significant (the statistical spread associated to the number of counts at the bottom of the scans is $<\pm 1.5\%$). The large shoulder effect appears to vary strongly with the penetration depth. It is also remarkable to note that the scan corresponding to a mean penetration depth of 370 Å exhibits a bump near the half-minimum; the half-width at half-minimum is hence not well defined.

The yield corresponding to the first maximum of the spectra registered at $\varphi_0=22'$, $\varphi_0=24'$, and $\varphi_0=32'$ is impressively higher than the random yield. This effect is illustrated by the angular scan of Fig. 8. This scan represents the maximum maximorum as a function of φ_0, i.e., the yield (normalized with respect to the random yield) for an energy window $\Delta E \simeq R_E$ centered on the first maximum following either the surface peak or the surface edge of the spectra. The half-width at half-minimum of this scan is very near to that measured on the scan of Fig. 4 but the shoulder effect is far more pronounced. The yield on the top of the shoulder is 60% higher than the random yield. The shoulder is also very wide and the mean yield averaged over the whole scan is near the random yield. Similar results were obtained for the (100) plane. In particular, in this case, in conditions identical to those of Fig. 4, $\psi_{1/2}=15'$, i.e., $\psi_{1/2}(110)/\psi_{1/2}(100) \simeq [D(110)/D(100)]^{1/2}$ (see Table III).

TABLE III. Results obtained for the (110) and (100) planes with 1.9-MeV ^{4}He beams.

	D (Å)	$D^{1/2}$ (Å$^{1/2}$)	$\psi_{1/2}$ [a] (min)	λ [b] (Å)
(110)	2.03	1.42	18	380
(100)	1.44	1.20	15	320
(110)/(100) ratios	1.414	1.19	1.20	1.19

[a] Measured for an angular scan integrating the yield corresponding to the first two peaks of an aligned spectrum (see Fig. 4).

[b] Extracted from the aligned spectra using stopping powers given by Ref. 22. $S_{r.i.}=0.054$ keV/Å, $S_{r.o.}=0.058$ keV/Å. The energy of the outcoming particle backscattered near the surface for detection at $\theta_{lab}=120°$ is $\simeq 1.5$ MeV.

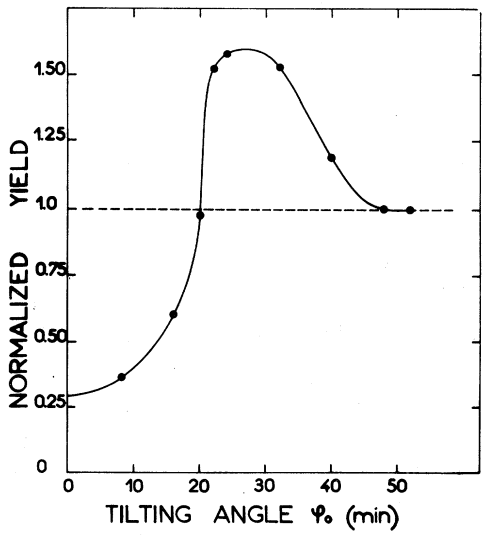

FIG. 8. Angular scan corresponding to the yield on the first maximum behind the surface peak or the surface edge of the spectra of Fig. 6.

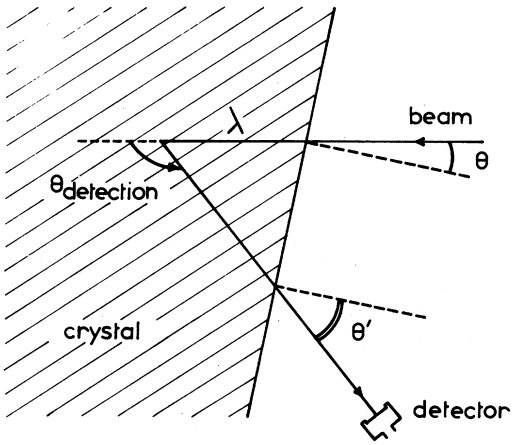

FIG. 9. Schematic representation of the geometry of a backscattering experiment.

C. Data reduction

In order to extract information from these results on the behavior of the particles in the crystal, the knowledge of a mean depth-energy relation is required. The energy spacing ΔE_λ between consecutive maxima in the energy spectrum corresponds to an increase of depth equal to λ and may be written

$$\Delta E_\lambda = \left(K\bar{S}_a + \frac{S_{r.o.}\cos\theta}{|\cos\theta'|} \right)\lambda , \tag{6}$$

where K is the backscattering kinematic coefficient, $S_{r.o.}$ is the random stopping power for the outcoming particles, and $\bar{S}_a$ is the mean (i.e., averaged over λ) stopping power along their way in the crystal of particles which are eventually backscattered. The angles θ and θ' are defined in Fig. 9, which schematizes the geometry of the backscattering experiments.

The values of λ and of the ratio $\bar{S}_a/S_{r.o.}$ have been calculated from the measurement of ΔE_λ in two experiments performed in the same conditions but for different values of the detection angle θ'. Indexing 1 and 2 the parameters which are varied between the first and the second experiment, one gets from Eq. (6),

$$\frac{\bar{S}_a}{S_{r.o.}} = \frac{\cos\theta(\Delta E_2/\cos\theta_2' - \Delta E_1/\cos\theta_1')}{K_2\Delta E_1 - K_1\Delta E_2} \tag{7}$$

and

$$\lambda = \frac{K_2\Delta E_1 - K_1\Delta E_2}{S_{r.o.}\cos\theta(K_2/\cos\theta_1' - K_1/\cos\theta_2')} . \tag{8}$$

The two experiments have been performed at the detection angles 120° and 165°. In spite of the calculated uncertainties corresponding to small errors on the measured ΔE_λ at the two emerging angles and of the uncertainties in the geometry itself, we could estimate the ratio $\bar{S}_a/S_{r.i.}$, where $S_{r.i.}$ is the random stopping power at the incoming particle energy, to be close to one for the (110) and (100) planes. This result is in good agreement with measurements from Poizat and Remillieux.[8] These authors found that the energy width of 2-MeV helium backscattering spectra on thin (600-Å) gold single crystals was nearly the same for "random" and planar-aligned spectra. Van der Weg *et al.*[9] extracted a value of the ratio $\bar{S}_a/S_{r.i.}$ varying from 4 to 5 in the case of the planar channeling of 120-KeV protons in Si. The fact that the value found by these authors is much higher than here might be due partly to the different particles and energies used in the two sets of experiments. On the other hand, the values found by these authors have been calculated by a rather indirect way and with very strong physical assumptions and approximations. The knowledge of the mean stopping power $\bar{S}_a$ does not give a precise information on the stopping power for particles in the region of their trajectories where they come close to the planes. However, the above estimation of $\bar{S}_a$ is most useful to calculate the mean oscillation half-wavelengths λ. We used a value of $\bar{S}_a$ equal to $S_{r.i.}$ in our calculations.

Values of S_r were extracted from the tables of Williamson *et al.*,[22] Ziegler *et al.*,[23] and Northcliff *et al.*[24] The corresponding values differ noticeably. Using, for instance, the stopping powers of Ref. 22 to calculate the energy to depth-conversion scales for the aligned spectra, we deduced a mean distance between two consecutive trajectory extrema, i.e., a mean half-wavelength λ, of 320 Å for the (100) plane and 380 Å for the (110) plane. Stopping powers from Ref. 23 would lead to $\lambda(110) = 330$ Å, i.e., a 15% discrepancy. As expected from relation (1), we found $\lambda(100)/\lambda(110) \simeq [D(100)/D(110)]^{1/2}$. The results are summarized in Table III.

DISCUSSION OF RESULTS

The discussion of the spectra presented in this work is, to a great extent, related to the concept of statistical equilibrium. The latter has been often assumed to be reached by the channeled particles over short distances, this assumption, combined to that of the approximate conservation of the transverse energy, leading to an easy calculation of the angular distribution of particles emerging from a crystal. These calculated blocking distributions have been directly compared to dips obtained in channeling experiments, the validity of the so-called reversibility principle being assumed. Let us first define, using the language of probability theory, what is precisely meant by "statistical equilibrium." Let $E_\perp$ and Y be the random variables corresponding to the transverse energy and to the

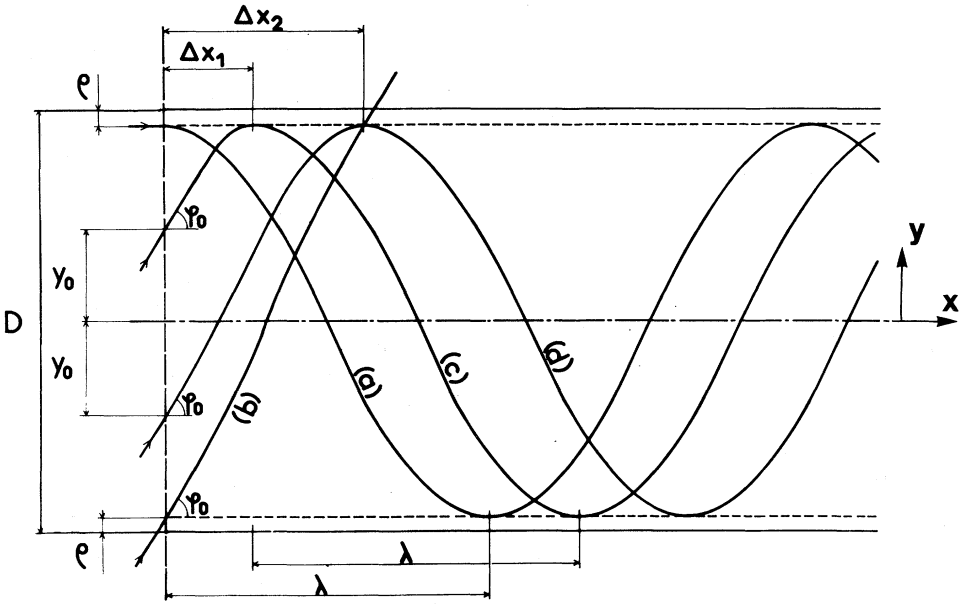

FIG. 10. Particle coordinates in the channel and schematic representation of trajectories for different entrance conditions. (a) $\varphi_0 = 0°$, $e_\perp^0 = e_\perp^c$; (b) $\varphi_0 = 28'$, $e_\perp^0 > e_\perp^c$; (c) and (d) $\varphi_0 = 28'$, $e_\perp^0 = e_\perp^c$. $\langle \Delta x \rangle = \frac{1}{2}(\Delta x_1 + \Delta x_2)$ is related to the shift towards low energies of the first maximum of the backscattering yield for $\varphi_0 \neq 0$.

distance to the center of the channel of a particle (see Fig. 10). The trajectories of the particles may be investigated by studying the probability laws with depth of $E_\perp$ and Y. In what follows, the potential in the planar channels will be called $V(y)$. η being the impact parameter and $U(\eta)$ the planar continuum potential associated to a single plane, we have

$$V(y) = U(\tfrac{1}{2}D + y) + U(\tfrac{1}{2}D - y) - 2U(\tfrac{1}{2}D) \ . \qquad (9)$$

Hence $V(0) = 0$. $U(\eta)$ presents, in fact, random fluctuations due to the correlated thermal vibrations of the lattice atoms. A particle entering the crystal at a distance $Y = y_0$ from the channel center has an entrance transverse energy $E_\perp^0 = e_\perp^0$ with

$$e_\perp^0 = E\varphi_0^2 + V(y_0) \ . \qquad (10)$$

We shall write $P(y \mid e_\perp^0; x)$ for the conditional probability density of Y being near y at depth x for a particle with entrance transverse energy $e_\perp^0$. We shall say that statistical equilibrium is reached at depth x_0 if $P(y \mid e_\perp^0; x)$ is independent of x for $x > x_0$, and this for all entrance transverse energies $e_\perp^0$. This condition may be formulated, considering the trajectories as random functions (rfs) $Y(x; e_\perp^0)$, by requiring $Y(x; e_\perp^0)$ to be stationary for $x > x_0$.

Figure 11 illustrates the meaning of statistical equilibrium; it shows the typical behavior of a random function $Y(x)$ with fixed initial values (φ_0 and y_0, equivalent to $E_\perp^0 = e_\perp^0$). $Y(x)$ was simulated electronically (Y being a signal amplitude and x equivalent to time) so as to have an oscillatory character with moderate statistical spread with time. The superposition of many traces gives a visual representation of $P(y \mid e_\perp^0; t)$; the distribution of the traces broadens slowly around its mean value which oscillates strongly, until the random phase shifts between the traces eventually mix them so as to lead to a distribution nearly uniform with time. It must be emphasized that statistical equilibrium has no meaning for a nonrandom process; it may only appear in channeling phenomena when multiple scattering has introduced a large enough random phase shift between trajectories characterized by the same initial transverse energy and hence impact parameter. For particles which come near to the planes, the random correlated thermal vibration of the atoms also con-

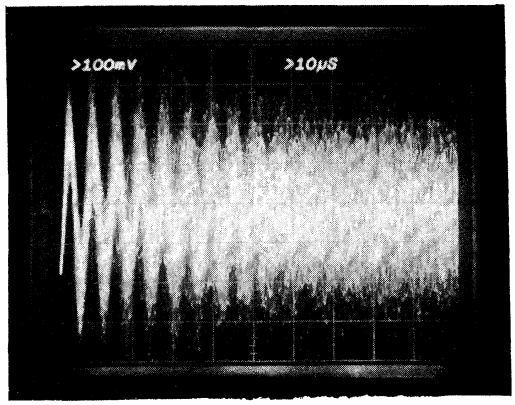

FIG. 11. Electronic simulation by a nearly periodical random function of a group of particles with identical entrance conditions. At the start the trajectories are well grouped around their oscillating mean value; the random phase shift soon lead to severe overlap until statistical equilibrium is approached.

tributes to the statistical effects by randomly perturbating the potential (this will be developed in more detail in Paper III).

It appears that the condition of a strict independence of $P(y|e_\perp^0; x)$ of x, if satisfied, implies the conservation of $E_\perp$ along the particle trajectory; if $E_\perp$ is not conserved, the domain available for Y broadens with depth in contradiction with the assumed stationarity. Thus, it is clear that strict stationarity cannot be reached, since $E_\perp$ increases slowly with depth, this being by definition the dechanneling process, which is known to take place. In fact, a strict conservation of $E_\perp$ would imply that

$$E_\perp = V(Y) + E(\dot{Y})^2 = E_\perp^0 , \tag{11}$$

where $\dot{Y} = dY/dx$. This is the ordinary differential equation [neglecting fluctuations of $V(y)$ of thermal origin] of a nonrandom periodic oscillating motion which allows for no multiple scattering and hence for no dechanneling effect.

A less stringent and more realistic definition of statistical equilibrium is thus that $P(y|e_\perp^0; x)$ varies slowly with x for $x > x_0$, i.e., that over a depth interval of the order of a mean half-wavelength λ, its variations with x are small; $E_\perp$ is then also assumed to vary slowly with depth. One of the questions which will be discussed here relates to the conclusions that may be drawn from the above results as to the speed with which statistical equilibrium is reached, if ever, in planar channeling phenomena.

In fact, the above experiments are directly related to the probability density $P(y; x)$ of $Y(x)$, which is proportional to the particle flux across the channel. The knowledge of $P(y; x)$ allows one to calculate the backscattering (or nuclear reaction, etc.) yield on the lattice atoms or on any impurity atom lying in a well defined position in a channel. The interpretation of all lattice-location experiments involves assumptions on $P(y; x)$. In particular if $P(y; x)$ varies smoothly with depth so does the backscattering spectrum with energy. We may readily write

$$P(y; x) = \int P(y|e_\perp^0; x) g(e_\perp^0)\, de_\perp^0 , \tag{12}$$

where $g(e_\perp^0)$ is the probability density of $E_\perp^0$. It is clear that the slow variation of $P(y|e_\perp^0; x)$ with x implies the same property for $P(y; x)$. *The converse is however not true*: $P(y; x)$ may be practically independent of depth while $P(y|e_\perp^0; x)$ still strongly oscillates with x. This is due to the mixing of the components of the integral of Eq. (12) for various $e_\perp^0$; in contrast with the case of $P(y|e_\perp^0; x)$, a trend towards uniformity of $P(y; x)$ with depth may be obtained even if $E_\perp$ is strictly conserved and if multiple scattering is neglected, because of the difference of wavelengths of the trajectories of particles of different entrance impact parameters, i.e., because of the nonharmonicity of the planar potential. This effect will be discussed and illustrated in the next paper of this series. Thus, it appears that the trend towards statistical equilibrium is much slower than the trend towards uniformity of $P(y; x)$, i.e., than the trend towards a smooth variation of the backscattering spectra with decreasing energy.

In conclusion, the fact that the strong maxima in the spectra damp out only after the sixth maximum, i.e., for depths larger than 5λ, indicates that $P(y; x)$ approaches uniformity only for $x > 5\lambda$ and that statistical equilibrium is reached, if ever, at depths much larger than 5λ, in this case for $x \gg 2000$ Å.

It is of interest to compare the experimental results presented here to calculations of planar angular scans, performed by Andersen[25] and Picraux *et al.*[26] The calculated angular scans exhibit strong shoulder effects. The existence of statistical equilibrium and the conservation of transverse energy are two of the main assumptions underlying these calculations. The experimental scans reported here (see Fig. 7) show in a striking way that the shoulder effect is only noticeable at penetration depths smaller than 1400 Å. These are depths where statistical equilibrium is obviously not reached, as clearly shown by the nonuniform yield observed on the portions of the spectra corresponding to this depth range. The scan recorded near penetration depths of 1400 Å where the yield in the spectra corresponding to large φ_0 becomes independent of energy (i.e., of depth) exhibits no shoulder effect. Taking into consideration the preceding conclusions the experimental results clearly prove that, at statistical equilibrium, the shoulder effect is certainly absent. The calculated angular scans of Refs. 25 and 26 could perhaps be compared to experimental scans by integrating the backscattering yield near the surface over depths of the order the oscillation wavelengths of the particles able to be backscattered. A typical example of this procedure is, in our case, the scan of Fig. 4. Such an integration could in a sense be considered as a simulation of statistical equilibrium. However, as will be shown in Paper II, a simulation of statistical equilibrium should consist in averaging the yield for each particle over one oscillation. The corresponding depth intervals are widely spread, especially when increasing φ_0 (see Paper II). So, no unique integration depth exists satisfying this requirement. The shape of the angular scans is hence very dependent of the integration depth and this parameter should clearly appear in any precise calculation or computer simulation of planar angular scans.

A basic result extracted from the spectra of Figs.

5 and 6 is the constancy of the energy separation between two consecutive maxima (except for the first two peaks) for spectra registered at different tilting angles φ_0 with respect to the plane. This result clearly suggests that the yield maxima are due to particles belonging to a well defined transverse energy interval and having hence trajectories characterized by a well defined interval of wavelengths centered on the mean half-wavelength λ. Considering the case of the aligned spectrum, it may be concluded that the transverse energy interval associated to these particles is necessarily centered just below the critical transverse energy for channeling $e_\perp^c$, which is of the order of $V(\frac{1}{2}D-\rho)$, ρ being the rms value of the thermal vibration amplitudes of the atoms perpendicular to the planes. The particles having a transverse energy in this interval have a motion which is still mainly determined by the planar potential but, in a part of their trajectories, they are close enough to the planes to have a high backscattering probability. The observation of planar channeling by backscattering leads thus to the *selection of precisely those particle groups* which present well defined, rather high transverse energies, whatever the value of φ_0. A detailed analysis of the spread of the corresponding half-wavelengths around λ will thus give information on the motion of the particles in the vicinity of the crystal planes. Such an analysis will be attempted in Papers II and III of this series.

While λ appears independent of φ_0, the first maximum of the spectra is shifted strongly towards lower energies with increasing φ_0. This may be explained considering Fig. 10 representing some typical trajectories. This figure illustrates the case of a tilting angle $\varphi_0 = 28'$. The particles of transverse energy near $e_\perp^c$ enter the crystal with small y_0, i.e., with great impact parameters η_0 with respect to the planes. The particles of smaller η_0 have transverse energies greater than $e_\perp^c$. They can cross the planes and their domain of pathlength between two consecutive planes is so wide that these particles will contribute to the backscattering spectrum by a uniform background. The particles of small y_0 can come near the planes and be backscattered only after a mean penetration depth $\langle \Delta x \rangle$. These particles will then stay close to the planes in a rather large depth interval enhancing the backscattering yield. This explains the great shoulder effect, i.e., the first maximum much higher than the random yield observed on the spectra of Fig. 6 for φ_0 near 28' (i.e., $\varphi_0 = 24'$ and $\varphi_0 = 32'$). The shift of this maximum towards low energies is of course related to the penetration depth $\langle \Delta x \rangle$. The particles contributing to this maximum have a transverse energy near $e_\perp^c$ and hence a mean half-wavelength λ. Consequently, they will contribute to other periodic maxima, the spacing between these maxima being, as discussed above, independent of φ_0. The results will be discussed more quantitatively in the following papers of this series, devoted to theoretical calculations.

ACKNOWLEDGMENTS

The authors wish to express their thanks to B. Thomas (IRSID) for providing the excellent Fe single crystals and to B. Agius for advice for electropolishing the samples. The efficient help of E. Girard for electronic problems and of J. Moulin in electromechanics, and especially in connection with the digitally controlled goniometer, was highly appreciated. The cooperation with C. Tourneville and J. Parizel for the design and construction of the goniometric chamber is gratefully acknowledged. The assistance of E. d'Artemare in problems related to the accelerator was most useful.

---

*Work supported by the Centre National de la Recherche Scientifique, Recherche Cooperative sur Programme n° 157.

[1]S. Datz, C. D. Moak, T. S. Noggle, B. R. Appleton, and H. O. Lutz, Phys. Rev. 179, 315 (1969).
[2]M. T. Robinson, Phys. Rev. 179, 327 (1969).
[3]M. J. Gaillard, J. C. Poizat, and J. Remillieux, Phys. Lett. A 45, 325 (1973).
[4]M. J. Gaillard, J. C. Poizat, J. Remillieux, F. Abel, M. Bruneaux, and C. Cohen, in *Atomic Collisions in Solids*, edited by S. Datz, B. R. Appleton, and C. D. Moak (Plenum, New York and London, 1975), Vol. 2, p. 779.
[5]E. Bøgh, Radiat. Eff. 12, 12 (1972)
[6]F. Abel, G. Amsel, M. Bruneaux, and C. Cohen, Phys. Lett. A 42, 165 (1972).
[7]F. Abel, G. Amsel, M. Bruneaux, and C. Cohen, C. R. Acad. Sci. (Paris) 276, 267 (1973).
[8]J. C. Poizat and J. Remillieux, thesis (Lyon, 1972) (unpublished).
[9]W. F. Van der Weg, H. E. A. Roosendaal, and W. H. Kool, Radiat. Eff. 17, 91 (1973).
[10]J. H. Barrett, Phys. Rev. B 3, 1527 (1971).
[11]J. H. Barrett, in Ref. 4, p. 841.
[12]D. V. Morgan and D. Van Vliet, in *Atomic Collisions in Solids IV*, edited by S. Andersen, K. Bjorkqvist, B. Domeij, and N. G. E. Johansson, (Gordon and Breach, London, New York, and Paris, 1972), p. 151.
[13]H. O. Carstanjen and R. Sizman, in Ref. 12, p. 173.
[14]R. D. Alexander and J. M. Poate, in Ref. 12, p. 159.
[15]F. H. Eisen and E. Uggerhøj, in Ref. 12, p. 181.
[16]C. Cohen, thesis (Paris, 1973) (unpublished).
[17]F. Abel, G. Amsel, M. Bruneaux, and C. Cohen, Ref. 4, p. 819.
[18]F. Abel, G. Amsel, M. Bruneaux and C. Cohen, Abstract, U. S.-Italy Seminar on Ion Beam Analysis,

Catania, Italy, June 1974 (unpublished).
[19]G. Amsel, J. P. Nadai, E. d'Artemare, D. David, E. Girard, and J. Moulin, Nucl. Inst. Meth. 92, 481 (1971).
[20]F. Abel, G. Amsel, M. Bruneaux, and C. Cohen, Radiat. Eff. 12, 35 (1972).
[21]B. Agius and J. Siejka, J. Electrochem. Soc. 120, 1019 (1973).
[22]C. F. Williamson, J. P. Boujot, and J. Picard, Rapport C. E. A. R3042, Saclay, 1966.
[23]J. F. Ziegler and W. K. Chu, Atom. Data Nucl. Data Tables 13, 463 (1974).
[24]R. C. Northcliffe and R. F. Schilling, Nucl. Data Tables A 7, 233 (1970).
[25]J. U. Andersen, Kgl. Danske Videnskab. Selskab, Mat. Fys. Medd. 36, 7 (1967).
[26]S. T. Picraux and J. U. Andersen, Phys. Rev. 186, 267 (1969).

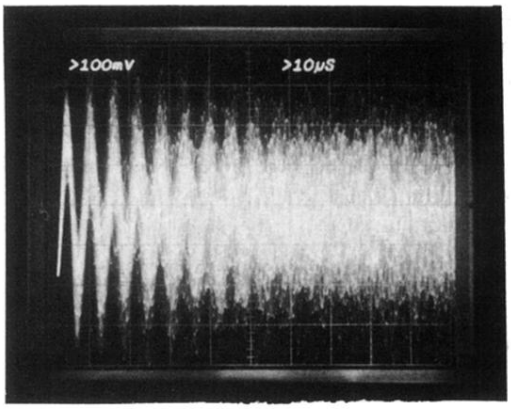

FIG. 11. Electronic simulation by a nearly periodical random function of a group of particles with identical entrance conditions. At the start the trajectories are well grouped around their oscillating mean value; the random phase shift soon lead to severe overlap until statistical equilibrium is approached.